ARTICLE
Journal of Cellular Biochemistry 106:16–24 (2009)

Journal of Cellular Biochemistry

Oncoprotein BMI-1 Induces the Malignant Transformation of HaCaT Cells

Qian Wang,[1] Wen-Lin Li,[1] Pu You,[1] Juan Su,[1] Ming-Hua Zhu,[2] Dong-Fu Xie,[1] Hai-Yin Zhu,[1] Zhi-Ying He,[1] Jian-Xiu Li,[1] Xiao-Yan Ding,[3] Xin Wang,[3,4] and Yi-Ping Hu[1*]

[1]*Department of Cell Biology, Second Military Medical University, Shanghai 200433, PR China*

[2]*Department of Pathology, ChangHai Hospital, Shanghai 200433, PR China*

[3]*Key Laboratory of Molecular & Cell Biology, Shanghai Institutes for Biological Sciences, Chinese Academy of Sciences, Shanghai 200031, PR China*

[4]*Stem Cell Institute, University of Minnesota, Minneapolis, Minnesota 55455*

ABSTRACT

BMI-1 (B-cell-specific Moloney murine leukemia virus integration site 1), a novel oncogene, has attracted much attention in recent years for its involvement in the initiation of a variety of tumors. Recent evidence showed that BMI-1 was highly expressed in neoplastic skin lesions. However, whether dysregulated BMI-1 expression is causal for the transformation of skin cells remains unknown. In this study, we stably expressed BMI-1 in a human keratinocyte cell line, HaCaT. The expression of wild-type BMI-1 induced the malignant transformation of HaCaT cells in vitro. More importantly, we found that expression of BMI-1 promoted formation of squamous cell carcinomas in vivo. Furthermore, we showed that BMI-1 expression led to the downregulation of tumore suppressors, such as p16INK4a and p14ARF, cell adhesion molecules, such as E-Cadherin, and differentiation related factor, such as KRT6. Therefore, our findings demonstrated that dysregulated BMI-1 could indeed lead to keratinocytes transformation and tumorigenesis, potentially through promoting cell cycle progression and increasing cell mobility. J. Cell. Biochem. 106: 16–24, 2009.

KEY WORDS: BMI-1; HaCaT CELL LINE; SKIN CANCER; MALIGNANT TRANSFORMATION

BMI-1(B-cell-specific Moloney murine leukemia virus integration site 1), a member of the polycomb group (PcG), is an epigenetic chromatin modifier with an essential role in embryogenesis [van der Lugt et al., 1994] and the maintenance of adult stem cells [Alkema et al., 1997; Molofsky et al., 2003; Park et al., 2003]. BMI-1 was first identified as an oncogene that cooperates with c-myc in the generation and development of mouse pre B-cell lymphomas [Haupt et al., 1991; van Lohuizen et al., 1991]. High expression of BMI-1 often associates with various malignancies, such as B-cell Hodgkin and non-Hodgkin lymphoma [Raaphorst et al., 2000; van Kemenade et al., 2001], mantle cell lymphoma [Beà et al., 2001; Visser et al., 2001], acute myeloid leukemia [Park et al., 2003], prostate cancer [Varambally et al., 2002], breast carcinoma [Al-Hajj et al., 2003], non-small cell lung cancer [Vonlanthen et al., 2001], medulloblastoma [Leung et al., 2004], colorectal cancer [Kim et al., 2004] and hepatocellular carcinoma [Wang et al., 2008]. BMI-1 has been shown to repress the expression of INK4a-ARF tumor suppressors by organizing chromosomes into a configuration inaccessible to transcription factors [Lindström et al., 2001]. The hypothesis that cancer is essentially a disease of stem cells is receiving increasing support, with the discovering of "cancer stem cells" in acute myeloid leukemia [Lapidot et al., 1994], chronic myeloid leukemia [Jamieson et al., 2004], breast cancer [Al-Hajj et al., 2003], and medulloblastoma [Singh et al., 2003]. BMI-1 was reported a critical determinant for the self-renewal of leukemic stem cells, as it in hematopoietic stem cells [Lessard and Sauvageau, 2003]. Recently, Chiba et al. [2007] found that overexpression of BMI-1 alone enhanced self-renewal capability in hepatic progenitor cells and induced their malignant transformation. Therefore, BMI-1 is currently regarded as a "stemness signature " in cancer cells.

Epithelial skin tumors are the most common human cancers. Although p53 mutations, chromosome instability, ras oncogene

Grant sponsor: National Natural Science Foundation of China; Grant numbers: 30470876, 30600326, 30472141; Grant sponsor: Chinese National 863 Project; Grant number: 2006AA02Z474; Grant sponsor: Shanghai Key Basic Science Project; Grant numbers: 03DJ14020, 06DJ14001.

*Correspondence to: Prof. Yi-Ping Hu, Department of Cell Biology, Second Military Medical University, Shanghai 200433, PR China. E-mail: yphu@smmu.edu.cn

Received 8 April 2008; Accepted 17 September 2008 • DOI 10.1002/jcb.21969 • 2008 Wiley-Liss, Inc.

Published online 19 November 2008 in Wiley InterScience (www.interscience.wiley.com).

mutations and virual infection have all shown to contribute to the development of such malignancies [Lacour, 2002; Ehrhart et al., 2003; Chiba et al., 2007], our understanding of the underlying mechanisms is still far from complete. Recently, BMI-1 overexpression was associated with in basal and squamous cell carcinomas [Reinisch et al., 2007]. However, it has not been established that BMI-1 expression causes keratinocyte transformation and skin cancer.

HaCaT (human skin keratinocytes) is a spontaneously immortalized keratinocyte cell line without detectable BMI-1 protein expression. HaCaT is a stable, non-tumorigenic keratinocyte cell line with largely preserved differentiation capacity. Such unique properties make HaCaT an excellent model for the study of the skin cancers originating from keratinocytes [Boukamp et al., 1988, 1990, 1997; Breitkreutz et al., 1991; Fusenig and Boukamp, 1998]. In this report, we stably transfected BMI-1 into HaCaT cell to generate HaCaT-BMI-1 cells. Using this cell, we demonstrated for the first time that expression of BMI-1 indeed led to keratinocyte transformation and skin cancer. In accordance with these findings, we showed that BMI-1 expression downregulated the expression of CDK inhibitors, cell adhesion molecules as well as cell differentiation factors. Thus, our results suggest that BMI-1 can cause skin cancer, potentially through promoting cell cycle progression and increasing cell mobility.

MATERIALS AND METHODS

VECTOR CONSTRUCTION, CELL CULTURE, AND TRANSFECTION

The HaCaT cell line (DKFZ) was derived from human skin keratinocytes spontaneously transformed in vitro during long-term incubation of a primary culture under selected culture conditions as described previously [Boukamp et al., 1988]. All cells were cultured in DMEM HG (Gibco BRL, MD) medium supplemented with 10% FBS (Hyclone, UT), 100 U/ml penicillin (Gibco BRL, MD), 100 μg/ml streptomycin (Gibco BRL) and 2 mM Glutamax (Gibco BRL) at 37°C with 5% CO_2. Subcultures were obtained by disaggregating the cells with 0.05% trypsin/EDTA solution and replating at a split ration of 1:10.

To construct pcDNA3.0-BMI-1, full-length human BMI-1 cDNA was amplified by the RT-PCR from the total RNA of one fresh human hepatocellular carcinoma tissue obtained from the Department of Pathology, Changhai hospital, Shanghai, PR China. by primers: 5′-AGCAGAAATGCATCGAACAA-3′ and 5′-CCTAACCAGATGAAGTTGCTGA-3′. The validity of the 989 bp fragment was confirmed by sequence after being cloned into the pUCm-T vector (Sangon, Shanghai). A *Not I*/*Bgl II* fragment containing BMI-1 cDNA was recovered from plasmid pUCm-T-BMI-1 and was subcloned into the *BamH I*/*Not I* digested pcDNA3.0 vector (Invitrogen, CA), which contains the neomycin gene. In this configuration, CMV immediate early promoter controlled the expression of BMI-1 protein. The recombinant plasmid pcDNA3.0-BMI-1 was introduced into the 35th passage HaCaT cells by electroporation. After 16 days selection by G418 (600 μg/ml), the individual G418 resistant clones were serially diluted and replated into a U bottom 96-well plastic tissue culture plates (1/2 cell in 200 μl culture medium per well). Cultured wells containing only one cell were marked (total 28 wells) and observed every 3 days under phase contrast microscopy. Upon reaching confluency, the clones from each well were dissociated and plated in 6-well plastic tissue culture plates (Geriner, Germany). Eventually four clones were selected and serially numbered as cloned HaCaT #1 ∼ #4. The negative control HaCaT-pcDNA3.0 was gained as the 35th passage HaCaT cells transfected with pcDNA3.0 according to above procedures.

GENOMIC DNA PCR AND RT-PCR ANALYSIS

All selected clones were examined individually for integration of the plasmids by using PCR to detect the exogenous BMI-1 cDNA in their genomic DNA. Genomic DNA from each clone was isolated by the sodium dodecyl sulfate lysis procedure described previously by Saxon et al. [1985]. The PCR conditions were 5 min at 95°C followed by 30 cycles of 1 min at 94°C, 1 min at 53.2°C, 1 min at 72°C and a final cycle at 72°C for 10 min. The primers were the same as the ones by which full-length human BMI-1 cDNA was amplified from the human hepatocellular carcinoma tissue.

Expression of the BMI-1 mRNA was analyzed by RT-PCR. Total RNA was extracted from HaCaT #1–#4, HaCaT-pcDNA3.0, parental HaCaT, fresh tumor and nontumorous tissues of 5 SCID mice by Trizol reagents (Invitrogen) according standard protocols. Reverse transcription was performed with 2 μg RNA, random nonamers (TaKaRa, Dalian) and M-MLV reverse transcriptase (Promega, WI) according to manufacturer's manual. The PCR primers and reactions specified for BMI-1 were same as described above. GAPDH was used as an internal quantitative control, the forward and reverse primers were 5′-GGTGGTCTCCTCTGACTTCAACA-3′ and 5′-GTTGCTGTAGCCAAATTCGTTGT-3′, with the annealing temperature of 58°C.

WESTERN BLOTTING AND IMMUNOCYTOCHEMISTRY

To confirm the expression of BMI-1 protein, the 2nd passage HaCaT #3, #4 and HaCaT-pcDNA3.0 were homogenated in a RIPA lysis buffer, and lysates were cleared by centrifugation (12,000 rpm) at 4°C for 10 min. About 150 μg protein samples were run on a 10% SDS–PAGE gel and transferred to polyvinylidine difluoride membranes (Bio-Rad, Hercules, CA). Membranes were blocked for 1 h in Tris-buffered saline with 0.05% Tween-20 (TBST) containing 5% skim milk and probed with the primary monoclonal antibodies directed toward BMI-1 (1:1,200) (ab14389, Abacam, Cambridge, UK), GAPDH (1:10,000) (10494-1-AP, Yeli bioscience Co., Ltd. Shanghai, PR China) respectively overnight at 4°C. The membranes were then washed three times with TBST for 10 min and incubated with HRP-conjugated Rabbit polyclonal anti-mouse secondary antibody (1:1,000) (Proteintech Group, Inc., Chicago) for 2 h at 37°C. After being washed three times, the membranes were immersed in diaminobenzidine (DAB) as substrates.

The 2nd passage HaCaT #3, #4 and HaCaT-pcDNA3.0, growing on poly-L-lysine-coated slide glasses, were fixed in 4% paraformaldehyde for 30 min. The cells were incubated with 5% goat serum to block the non-specific binding sites. Mouse monoclonal anti-BMI-1 (1:200) (ab14389, Abacam, Cambridge, UK) antibody was used as primary antibody. The cells were incubated with the first antibody for 2 h at 37°C, and then stained with the Dako Envision detection system (Dako, CA).

For further observation of the cellular morphology change, the 2nd passage HaCaT #3, #4, HaCaT-pcDNA3.0 and parental HaCaT, growing on poly-L-lysine-coated slide glasses, were fixed in the mixed solution of methanol and ethanoic acid (3:1) for 30 min, then stained with Giemsa for 15 min.

PROLIFERATION CURVE IN VITRO

Cell proliferation and cell death were assessed using Trypan blue staining. The 2nd passage HaCaT #3 and #4 cells were plated into a 24-well plastic tissue culture plate (Geriner) according to 1×10^4 cells per well. The cultures were grown for 7 days. The cells of every three wells were trypsinized for enumerating the number of viable cells separately each day. The cells of each well were enumerated triplicately and the average number of three wells was recognized as the means daily. Cell doubling time was calculated as the formular $TD = t \log 2/\log(N/N_0)$. The growth curves of HaCaT-pcDNA3.0 and parental HaCaT were also displayed as the same process.

ANCHORAGE-INDEPENDENT COLONY FORMATION ASSAY

The 2nd passage HaCaT #3 and #4 cells were separately plated into soft agar (Wako, Osaka, Japan) in a 24-well plastic tissue culture plate (Geriner) according to 25, 50, and 100 cells per well. The cells were suspended in 800 μl of 0.35% agar supplemented with the culture medium. The cell suspension was layered over the bottom layer of 800 μl of 0.6% agar. HaCaT-pcDNA3.0 and parental HaCaT were treated with the same method. Colonies >50 μm in diameter were counted in triplicate wells at day 21 of culture.

TUMORIGENICITY TEST AND HISTOLOGIC ANALYSIS

A total of 1×10^8 cells derived from the 2nd passage HaCaT #3 or #4 cells were suspended in 1 ml DMEM HG medium with 10% FBS and injected subcutaneously into the right inguina of SCID mice (3 weeks old) under anesthesia. The same amount of HaCaT-pcDNA3.0 cells were suspended in the same way and injected subcutaneously into the left inguina of SCID mice. The animals were kept for an observation period of up to 5 weeks and the injection sites were palpated weekly. Tumor nodules were removed, fixed in 4% phosphate-buffered paraformaldehyde overnight at 4°C, embedded in OCT compound and prepared for cryostat sections in 8 μm. The frozen sections of murine tumors were stained with H&E for pathologic analysis. They were also used for immunohistochemical analysis. The sections were treated with 1% hydrogen peroxide in methanol to quench the endogenous peroxidase activity, followed by incubation with 1% BSA to block the non-specific binding and stained with anti-BMI-1 (1:120) as described previously. After reacted with the secondary antibody described previously, the tissue sections were immersed in diaminobenzidine (DAB) as substrates.

REAL-TIME RT-PCR

Total cellular RNA was extracted from the 2nd passage HaCaT #3, #4 and HaCaT-pcDNA3.0 by using Trizol (Invitrogen, CA) following the manufacturer's instructions. cDNA was generated by using 2 μg RNA and the procedure of reverse transcription was described previously. Reactions were conducted using an iCycler iQ real-time PCR detection system (Bio-Rad) with SYBR Green I fluorescent dye (TOYOBO, Japan). A twofold change threshold was used to determine regulated genes. The comparative threshold cycle (C_T) method against the expression level of GAPDH was used to determine relative quantities. Primers used are listed Table I.

STATISTICS

Data represent means ± SEMs. Statistical differences between groups were analyzed using the Fisher's exact test. Differences were considered significant at $P < 0.05$. All statistical analyses were performed using the SAS^R software package (version 8.01, SAS Institute, Cary, NC).

RESULTS

MORPHOLOGY CHANGE OF ESTABLISHED HaCaT-BMI-1 CELLS

BMI-1 cDNA was PCR cloned from human hepatocellular carcinoma tissue. The correct clones, which encoded wild type BMI-1 (NC_000010.9), were identified by sequencing analysis. Four drug resistant cell lines were obtained by transfecting BMI-1 cDNA into HaCaT cells (passage 35). By PCR analysis, cell lines #3 and #4 were identified to contain exogenous BMI-1 cDNA. In addition, mRNA transcribed from integrated vector was detected by RT-PCR in cell lines #3 and #4 as well (Fig. 1A,B). BMI-1 protein was also detected in cell lines #3 and #4 by Western blotting and immunocytochemistry analysis (Fig. 1C,D). Cell lines #3 and #4 referred to as HaCaT-BMI-1 #3 and HaCaT-BMI-1 #4 in the later text were therefore used for further studies. In HaCaT-BMI-1 cells, including HaCaT-BMI-1 #3 and #4 cells, BMI-1 protein was found specifically localized to the peri-nucleus region (Fig. 1D). Further passaged HaCaT-BMI-1 cells lost characteristic cobblestone morphology to exhibit a lumping phenotype with an increased nuclear-to-cytoplasm ratio when cultured in DMEM HG medium with 10% FBS at 37°C, 5% CO_2. Nonetheless, no typical polynucleus and nuclear atypia were observed in HaCaT-BMI-1 cells. The number of nucleoli and chromatin spots in HaCaT-BMI-1 was similar to that of negative

TABLE I. Primer Sequences Used

E-Cadherin	5′-TTCTGCTGCTCTTGCTGTTT-3′
	5′-CAGGACTTTGACTTGAGCCA-3′
p14ARF	5′-CGCTCTGGCTTTCGTGAAC-3′
	5′-GTGAACGTTGCCCATCATCA-3′
P16	5′-CAGGGCCGTGTGCATGAC-3′
	5′-AGTTCGAATCTGCACCGTAGTTG-3′
KRT6	5′-CAGATCAAGGCGCTAAACAA-3′
	5′-CTCATAAATGGGCTCCAGGT-3′
CCND1	5′-AACAAACAGATCATCCGCAA-3′
	5′-ACTCTGGAGAGGAAGCGTGT-3′
CCNE1	5′-ACAGATTGCAGAGCTGTTGG-3′
	5′-ATGGAACCATCCACTTGACA-3′
CCNA2	5′-GCTATCCTCGTGGACTGGTT-3′
	5′-AGGCTAACAGCATAGCAGCA-3′
CDKN1A	5′-CAGGCTTCGCTCTATCTTCC-3′
	5′-CCCACATGAATCGTATGCTC-3′
CDKN2C	5′-TACAGCAGAAAGCCTGAACG-3′
	5′-AAGGAGAGTGATGCGGAAAG-3′
CDKN1C	5′-ATCCACGATGGAGCGTCT-3′
	5′-TGTCCTGCTGGAAGTCGTAA-3′
GAPDH	5′-GGTGGTCTCCTCTGACTTCAACA-3′
	5′-GTTGCTGTAGCCAAATTCGTTGT-3′

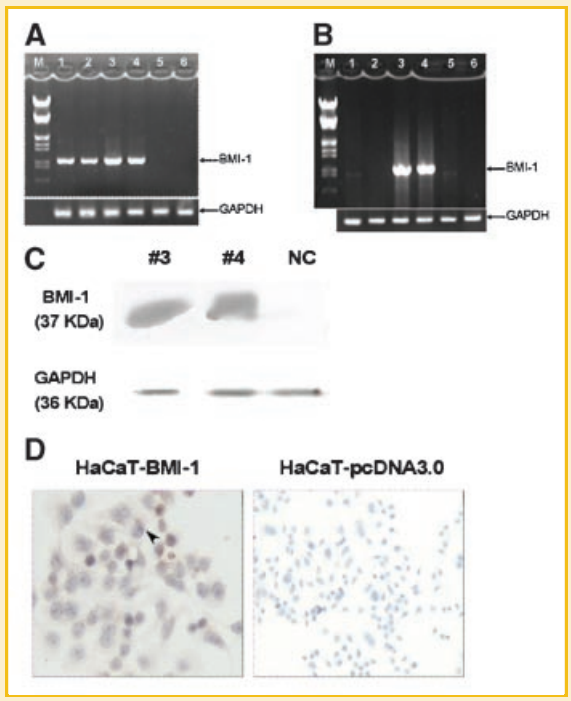

Fig. 1. Establishment of HaCaT-BMI-1 cell lines by transduction of BMI-1 in HaCaT cells. A: BMI-1 transcript expression was assessed by RT-PCR. All selected monoclones transfected with pcDNA3.0-BMI-1 vector expressed BMI-1 mRNA. B: Integration status of exogenous BMI-1 cDNA was assessed by genomic DNA PCR. Only in HaCaT #3 and HaCaT #4 cell lines, BMI-1 cDNA integration was detected. 1–4, HaCaT #1–#4. 5, HaCaT-pcDNA3.0. 6, parental HaCaT. GAPDH was used as a reference gene. C: BMI-1 expression was assessed by Western blot. BMI-1 protein can be detected from the cell extract of HaCaT #3 and HaCaT #4 cells. HaCaT #3 and HaCaT #4 were named as HaCaT-BMI-1 #3 and HaCaT-BMI-1 #4 cell lines. #3, HaCaT-BMI-1 #3. #4, HaCaT-BMI-1 #4. NC, HaCaT-pcDNA3.0 as a negative control. GAPDH served as a loading control. D: Immunocytochemical analysis was performed to identify the expression of BMI-1 further. HaCaT-BMI-1 cells were typical nuclear staining with BMI-1 (brown). Arrow indicates that BMI-1 localized to the nuclear rim of a positive cell. Magnification: D (200×).

control HaCaT-pcDNA3.0 cells as well as parental HaCaT cells (Fig. 2).

ENHANCEMENT OF PROLIFERATIVE CAPABILITY IN HaCaT-BMI-1 CELLS

To examine the effect of BMI-1 expression on the proliferation of HaCaT cells, we monitored the growth curve for HaCaT-BMI-1 #3, #4, HaCaT-pcDNA3.0 and parental HaCaT cells. Growth curves were plotted over a period of 7 days. It showed that BMI-1 enhanced the proliferation of HaCaT cells prominently in vitro. HaCaT-BMI-1 #3 and #4 cells displayed a similar result, they entered exponential phase of growth after being cultured for 48 h with a doubling time of 18 h, whereas HaCaT-pcDNA3.0 cells and parental HaCaT cells entered exponential phase of growth after being cultured for 72 h with a similar doubling time of approximately 24 h (Fig. 3). While HaCaT-pcDNA3.0 and parental cells stopped proliferate after 7 passages, HaCaT-BMI-1 cells did not stop proliferating until the 14th passage.

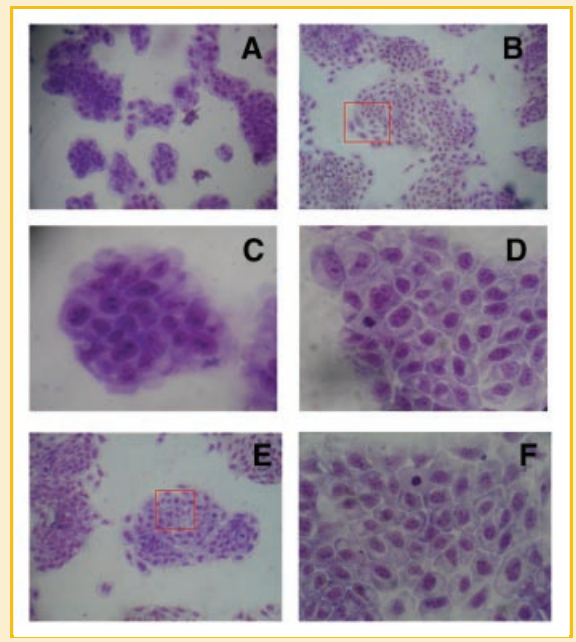

Fig. 2. Effect of BMI-1 oncoprotein on cell morphology in HaCaT cells. The morphology of HaCaT-BMI-1 #3 and HaCaT-BMI-1 #4 was similar, so we used HaCaT-BMI-1 cells as representative of the two cell lines. HaCaT-BMI-1 (A,C), HaCaT-pcDNA3.0 (B,D) and parental HaCaT (E,F) cells cultured in DMEM HG medium with 10% FBS were fixed and stained with Giemsa. A: Transduction of BMI-1 into HaCaT cells showed a "lumping" appearance. Frame C is a magnification of the outlined area in (A). HaCaT-BMI-1 cells exhibited a pile up appearance. B,E: HaCaT-pcDNA3.0 and parental HaCaT showed a similar cobblestone fashion. Panels D and F are magnifications of the outlined areas in Panels B and E, respectively. Relative magnification: A,B,E (100×) and C,D,F (400×).

NEOPLASTIC TRANSFORMATION OF HaCaT-BMI-1 CELLS IN CULTURE AND IN VIVO

While the HaCaT-pcDNA3.0 and parental cells maintained their contact inhibition ability, HaCaT-BMI-1 cells were defective in contact inhibition. The "pile-up" appearance of the HaCaT-BMI-1 colonies (Fig. 2A,C) prompted us to examine their anchorage-independent growth in soft agar. We seeded HaCaT-BMI-1 #3 and #4 cells separately in soft agar at the density of 25, 50, 100 cells per well and the same procedures were also performed using HaCaT-pcDNA3.0 and parental HaCaT cells in parallel as controls. After incubation for 3 weeks, in contrast to that no colonies were found in control cells, nearly 3% of the cells expressing BMI-1 formed large colonies and there was no significant difference in the various numbers of seeded cells (Fig. 4), indicating that BMI-1 expression promoted the transformation of HaCaT-BMI-1 cells in culture. To confirm these findings in vivo, we injected these three cell lines into SCID mice. All mice transplanted with HaCaT-BMI-1 #3 or #4 cells exhibited a similar course of tumor development and formed tumors at the size of 1–2 cm in diameter within 5 weeks after the injection (Fig. 5A,B). Histologic analysis of tumors derived from HaCaT-BMI-1 cells revealed nodular proliferation of highly differentiated squamous cell carcinoma. Tumor nodules were encapsulated and surrounded by mouse mesenchyme. Epidermis-like epithelium cells

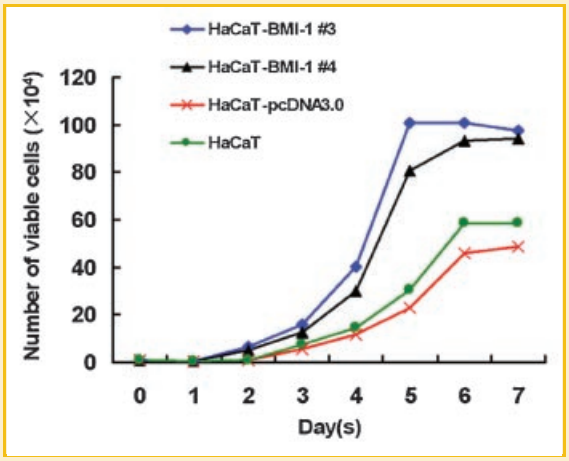

Fig. 3. Stably expression of BMI-1 promotes the proliferation of HaCaT cells in vitro. Growth curves of HaCaT-BMI-1 #3, HaCaT-BMI-1 #4, HaCaT-pcDNA3.0 and parental HaCaT cells are presented. The growth curves were determined in triplicate, and they are representative of three independent experiments. [Color figure can be viewed in the online issue, which is available at www.interscience.wiley.com.]

were found hyperplasia and derangement within these tissues. The cells exhibited no clear border and showed evident nuclear atypia such as nuclear enlargement, irregularities of the nuclear membrane, and nuclear pleomorphism. Neovascularization was also found in these tissues (Fig. 5C,D). BMI-1 mRNA was readily detected in these tumors compared with the nontumorous tissues adjacent to the tumors by RT-PCR (Fig. 5E). Immunohistochemical analysis revealed that BMI-1 specifically localized in the nuclear of the expressing cells insider the tumors. Unexpectedly, only approximate 30% cells of all the cells in a tissue section were positive for BMI-1, and nearly all of them clustered around the vessels (Fig. 5F,G). This result was similar to what reported in hepatocelluar carcinoma.

REPRESSION OF INK4A-ARF PATHWAY IN HaCaT-BMI-1 CELLS

It has been reported that the INK4a-ARF locus is a critical downstream target of BMI-1, which may contribute to cell cycle regulation and senescence by acting as a transcriptional repressor of the INK4a-ARF locus. p16INK4a and p14ARF, which prevent the inactivation and degradation of pRB and p53 respectively, are cell cycle inhibitors and major tumor suppressor proteins [Pomerantz et al., 1998; Lipinski and Jacks, 1999; Weber et al., 1999]. The correlation between the expression of BMI-1 in association with INK4a-ARF pathway in the genesis of colorectal carcinoma, lymphoma and leukemia has been reported [Park et al., 2004]. However, little is known whether BMI-1 regulates the expression of INK4a or other genes in keratinocytes. Assayed by quantitative real-time PCR, compared with HaCaT-pcDNA3.0 or HaCaT parental cells, HaCaT-BMI-1 #3 and #4 cells all expressed lower levels of p14ARF, p16INK4a, CDKN1A, KRT6, E-Cadherin, higher levels of CCND1, CCNE1, CCNA2, and similar levels of CDKN2C, CDKN1C (Fig. 6). Thus INK4a-ARF pathway was repressed in HaCaT-BMI-1 cells and the downstream cyclins were activated accordingly, which correlated with the enhanced proliferation of HaCaT-BMI-1 cells. In addition, downregulation of adhesion molecule E-Cadherin and differentiation related factor KRT6 could promote the malignant transformation of HaCaT-BMI-1 cells.

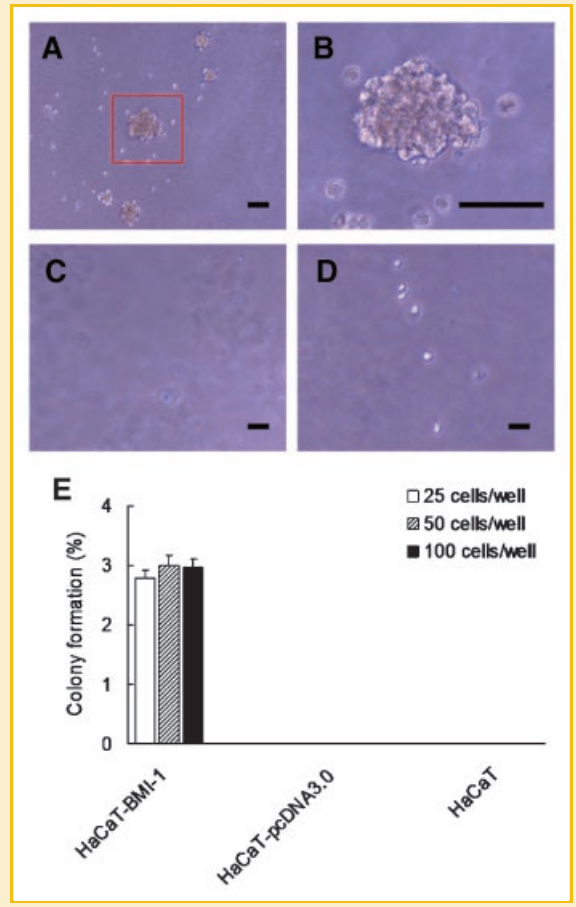

Fig. 4. Anchorage-independent colony formation in soft agar. A,B: Cells originated from HaCaT-BMI-1 can form colonies in soft agar. (B) is a magnification of the outlined area in (A). C: Cells from HaCaT-pcDNA3.0 cannot form colonies in soft agar. D: Cells from parental HaCaT cannot form colonies either. E: The percentage of anchorage independent colonies >50 μm in diameter after incubation for 21 days, that originated from HaCaT-BMI-1 seeded to a density of 25, 50, 100 cells per well was 2.80 ± 1.15, 3.00 ± 1.70, and 2.96 ± 1.50, respectively. The data represents the mean ± standard deviation of triplicate samples and the difference were no significant ($P < 0.05$). Magnification: A,C,D (100×) and B (400×). Scale bar, 50 μm. [Color figure can be viewed in the online issue, which is available at www.interscience.wiley.com.]

DISCUSSION

The BMI-1 gene, which is homologous to certain Drosophila Polycomb group genes, has been found to contribute to the development of body structure as well as the maintenance of adult stem cells self-renewal both in vitro and in vivo [van der Lugt et al., 1994; Molofsky et al., 2003; Park et al., 2003]. However, aberrant expression of BMI-1 protein also plays an important role in the initiation and progression of tumors. Despite the wealthy

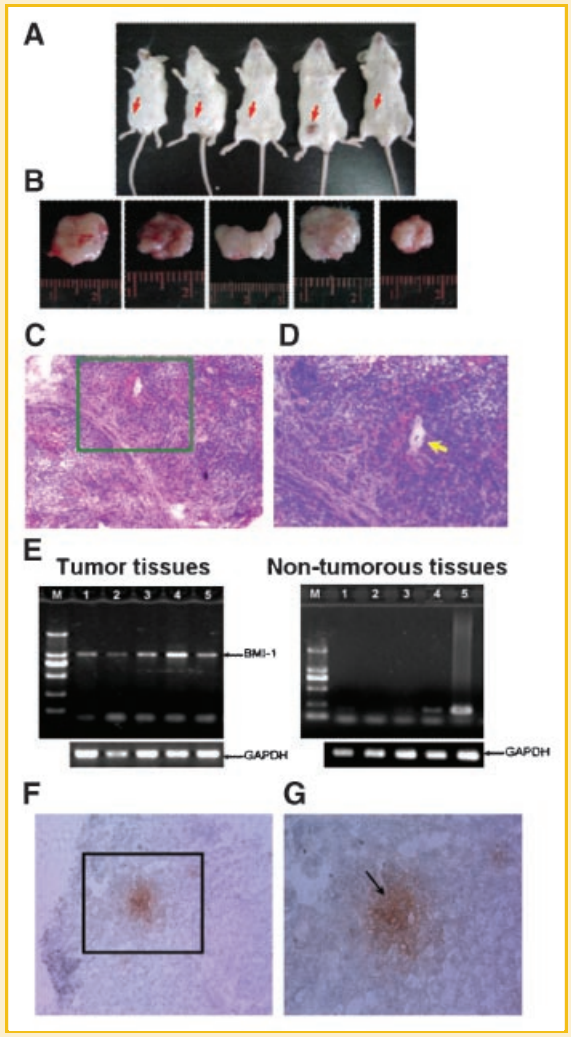

Fig. 5. Tumors derived from HaCaT-BMI-1 cells. A: Representative subcutaneous tumor was indicated (arrow) in the right inguina of SCID mice after subcutaneous injection of 1×10^8 HaCaT-BMI-1 #3 or #4 cells. No tumor was observed in the left inguina where injected the same amount of HaCaT-pcDNA3.0 cells. B: The tumors were dissected 5 weeks after the injection of 1×10^8 HaCaT-BMI-1 #3 or #4 cells. Scale unite of bar, cm. C,D: The frozen sections of tumor tissues were stained with hematoxylin–eosin. Histological analysis revealed that highly differentiated squamous cell carcinoma was formed and surrounded by mouse mesenchyme. Panel D is a magnification of the outlined area in Panel C. Arrowhead indicates angiogenesis in tumors. E: RT-PCR analysis confirmed BMI-1 gene expressed in all five tumors derived from HaCaT-BMI-1 cells but the expression was not detected in the non-tumorous tissues adjacent to the tumors. GAPDH was used as a reference gene. F: Immunohistochemical analysis revealed that the tumors consisted of BMI-1 positive cells (brown). G: is a magnification of the outlined area in (F). Arrowhead indicates the carcinoma cells distinct staining of BMI-1 protein surrounded a vessel. Original magnification: C,F (100×) and D,G (200×).

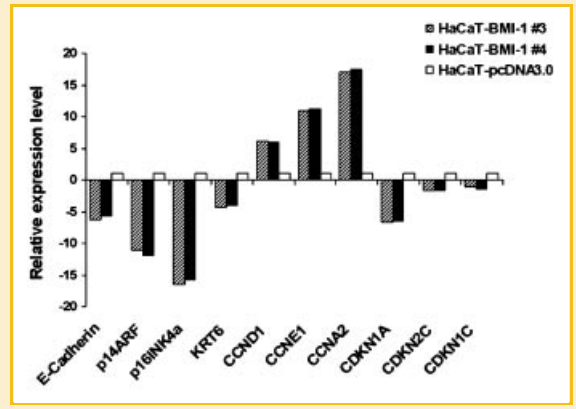

Fig. 6. Comparative expression level analysis for ten genes in HaCaT-BMI-1 #3, #4 and HaCaT-pcDNA3.0 by real-time RT-PCR. Expression levels were displayed as a ratio between the signal strength of a detected gene and the reference gene (GAPDH) to compensate for the variation in the amounts of RNA. The ratio of each gene in HaCaT-pcDNA3.0 was set at 1 and the relative fold change of the corresponding gene in HaCaT-BMI-1 #3 and #4 was showed. Values are the mean of triplicate reactions.

information on BMI-1 contributing to a variety of tumors, such as lymphomas, acute myeloid leukemia, breast cancers and hepatomas, its function on skin cancers remains poorly understood. The existence of BMI-1 positive cells in basal and squamous cell carcinomas has been reported by Reinisch et al. [2007] recently. We hypothesized that expression of BMI-1 in keratinocytes would lead to and promote its transformation and tumorigenic ability. To test this hypothesis, we first established two keratinocyte cell lines, HaCaT-BMI-1 #3 and HaCaT-BMI-1 #4. They both stably expressing BMI-1 protein and induced malignant transformation of spontaneously immortalized keratinocyte cell line HaCaT by repressing INK4a-ARF pathway. So we found that BMI-1 promotes neoplastic transformation of keratinocytes and may induce the genesis of human skin cancers.

BMI-1 is implicated in stable maintenance of gene repression and recognized, by means of interacting with histone methyltransferases, histones, and counteracting SWI/SNF-chromatin-remodeling complexes to form a repressive inaccessible chromatin structure which inhibits the transcriptional activity of target genes, among which senescence-associated genes are the best known to promote cell proliferation as well as to prevent cell senescence [Brock et al., 2001; Francis and Kingston, 2001; Ringrose and Paro, 2001]. In our experiments, BMI-1 stable expression endowed the HaCaT-BMI-1 cells with a prolonged proliferative advantage not only in vitro (Fig. 3) but also in vivo. Compared with parental HaCaT cells, HaCaT-BMI-1 proliferated in subcutis of SCID mice and developed tumors (Fig. 5A). Intriguingly, HaCaT-BMI-1 cells could form highly differentiated squamous cell carcinomas (Fig. 5C), although differentiation marker KRT6 decreased fourfold relative to the control HaCaT-pcDNA3.0 (Fig. 6). This result indicates that BMI-1 might not affect the differentiation capability of HaCaT cells. It is consistent with the finding that BMI-1 promotes cell proliferation without preventing their differentiation in hematopoietic stem cells and neuronal stem cells [Molofsky et al., 2003; Park et al., 2003]. In recent study, BMI-1 was reported positive staining in well/moderately differentiated hepatocellular carcinoma, but weakly or undetectable in poorly differentiated hepatocellular carcinoma. These results suggested that BMI-1 might play a role in the early stages of hepatocarcinogenesis, but not in the advanced carcinoma [Wang et al., 2008]. Reinisch et al. [2007] did not describe the

differentiation level of basal and squamous cell carcinomas containing BMI-1 positive cells, our results indict that BMI-1 may only enhance the proliferative capability of HaCaT cells both in vitro and in vivo, but did not prohibit their differentiation in vivo according to the transplantation experiment shown. The down-regulation of KRT6 might be a secondary change following with neoplasic transformation of HaCaT-BMI-1 cells, but not a direct target affected by BMI-1. It is generally accepted that the key event driving carcinogenesis is the spontaneous development of deregulated proliferation and reduced cell death. So we proposed dysregulated expression of BMI-1 might be an early event in promoting the transformation of normal keratinocytes to neoplasm. The more detailed information about differentiation of HaCaT-BMI-1 is currently under investigation in the surface transplantation model [Fusenig, 1994; Breitkreutz et al., 1997].

Unlike transformed fibroblast cells, there were no remarkable morphology changes in HaCaT-BMI-1 cells compared with parental HaCaT cells. The transformed HaCaT-BMI-1 cells did not exhibit typically malignant phenotype such as nuclear atypia, pathologic karyokinesis and nuclear pleomorphism (Fig. 2). This manifestation was similar to those observed in other experiments about transformed keratinocytes [Fusenig et al., 1983, 1985; Boukamp et al., 1990]. But the facts that HaCaT-BMI-1 cells exhibited ''pile-up'' appearance and possessed the characteristics of anchorage-independent growth (Fig. 4) demonstrated that HaCaT-BMI-1 cells were transformed in culture. These results supported our hypothesis that HaCaT-BMI-1 cells were just in the early stages of tumorigenesis, but not in the advanced stages. Unexpectedly, only 30% of all tumor cell population were positive for BMI-1 in squamouse cell carcinomas formed by HaCaT-BMI-1 cells (Fig. 5F), which was in accordance with the observations in hepatocellular carcinomas and skin cancers [Reinisch et al., 2007]. In the recent study performed by Chiba et al. [2007] overexpression of BMI-1 enhanced self-renewal of hepatic stem/progenitor cells and drives transformation of hepatic stem/progenitor cells specifically. They considered that human hepatocellular carcinoma originated from the hepatic stem/progenitor cells with abnormal expression of BMI-1. In leukemias, leukemia stem cells with increased expression of BMI-1 were also found essential for the initiation and development of tumors [Lessard and Sauvageau, 2003]. In terms of the opinion that an excessive and persistent growth signal is one of the key events in the initial stages of carcinogenesis [Wicha et al., 2006], we thought that in the highly differentiated squamous cell carcinomas derived from HaCaT-BMI-1 cells, the BMI-1 positive cells might be the initial cells with growth advantage and play a crucial role in the oncogenic process. Otherwise, BMI-1 was also reported as a novel tumor-associated antigen. Several CD8+ T-cell epitopes derived from BMI-1 were identified and could elicit interferon-γ (IFN-γ) release. So the phenomenon that most of the BMI-1 positive cells clustered around the vessels (Fig. 5G) might be associated with their immunogenicity. The BMI-1 protein might also represented a promising target antigen for cancer immunotherapy.

At present, BMI-1 protein has been found to induce tumors by means of the following two mechanisms: (1) in human mammary epithelial cells, BMI-1 induces telomerase directly or indirectly to immortalize epithelial cells and plays a role in the development of human breast cancer, but it fails to induce telomerase in fibroblasts [Dimri et al., 2002]; (2) in the studies of lymphomas [Lindström et al., 2001], leukemias [Lessard and Sauvageau, 2003], non-small cell lung cancers [Vonlanthen et al., 2001] and colorectal cancers [Kim et al., 2004], BMI-1 acts as a transcriptional repressor of the INK4a-ARF locus. Because HaCaT is a immortalized cell line in which telomerase is activated [Fusenig and Boukamp, 1998], we wanted to know whether INK4a-ARF locus was effected by BMI-1 in transformed HaCaT-BMI-1 cells. By real-time RT-PCR analysis, the mRNA expression level of p14ARF and p16INK4a in HaCaT-BMI-1 decreased 11- and 17-fold respectively relative to the control HaCaT-pcDNA3.0 and the downstream cyclins such as CCND1, CCNE1 and CCNA2 were increased accordingly (Fig. 6). Therefore, in our study, overexpression of BMI-1 markedly repressed expression of p14ARF and p16INK4a in HaCaT-BMI-1 cells. p14ARF and p16INK4a are encoded by the INK4a-ARF locus mapped to the chromosomal location 9p21, but are structurally unrelated [Lukas et al., 1995; Zhang et al., 1998]. p16INK4a inhibits cyclinD-Cdk4/6 kinase activities and thus the activation of E2F transcription factors, whose activities are critical for the G1/S transition [Sharpless and DePinho, 1999]. p14ARF binds MDM2 and thereby inhibits degradation of the p53 transcription factor. This results in activation of p53 target genes, leading to cell cycle arrest and apoptosis [Lowe and Sherr, 2003]. Both p14ARF and p16INK4a expression can be induced by aberrant mitogenic or oncogenic signaling, thus functioning as a potent fail-safe mechanism preventing cells from engaging in uncontrolled proliferation. Repression of INK4a-ARF pathway results evasion of apoptosis and limitless replication that disrupt the balance between the activity of cell growth and apoptotic signaling pathways, which are interdependent, and then induces unconstrained cell proliferation which is the predominant cellular event necessary for the development of cancer. Overexpression of BMI-1 or deletion of p14ARF and p16INK4a are frequently found in many types of human cancers, which implicates that they may collaboratively function as key regulators of immortalization or senescence checkpoints. As confirming evidence, our experiments showed that high level expression of BMI-1 led to excessive growth of HaCaT-BMI-1 cells by repressed INK4a-ARF pathway, thereby driving the initiation of cancer. Yet, the precise molecular mechanism of BMI-1 in the tumorigenesis of skin cancers remains to be further elucidated.

In conclusion, our experiments have demonstrated that increased BMI-1 oncoprotein expression could induce malignant transformation of HaCaT cells for the first time and strongly suggested that BMI-1 might promote neoplastic transformation of skin keratinocytes by means of repressing INK4a-ARF signaling pathway. In this regard, BMI-1 might be a potential target for novel therapeutic approaches against human skin cancers. In addition, we established a novel model for studying the molecular mechanisms of human skin cancers. It will facilitate our further understanding of the mechanism of cell transformation and tumorigenesis of skin cancers.

ACKNOWLEDGMENTS

We thank Dr. Yisong Wan, Department of Immunobiology, Yale School of Medicine, for his helpful suggestions and critique of the paper.

REFERENCES

Al-Hajj M, Wicha MS, Benito-Hernandez A, Morrison SJ, Clarke MF. 2003. Prospective identification of tumorigenic breast cancer cells. Proc Natl Acad Sci USA 100:3983–3988.

Alkema MJ, Bronk M, Verhoeven E, Otte A, van't Veer LJ, Berns A, van Lohuizen M. 1997. Identification of Bmi-1 interacting proteins as constituents of a multimeric mammalian polycomb complex. Genes Dev 11:226–240.

Beà S, Tort F, Pinyol M, Puig X, Hernández L, Hernández S, Fernandez PL, van Lohuizen M, Colomer D, Campo E. 2001. BMI-1 gene amplification and overexpression in hematological malignancies occur mainly in mantle cell lymphomas. Cancer Res 61:2409–2412.

Boukamp P, Petrussevska RT, Breitkreutz D, Hornung J, Markham A, Fusenig NE. 1988. Normal keratinization in a spontaneously immortalized aneuploid human keratinocyte cell line. J Cell Biol 106:761–771.

Boukamp P, Stanbridge EJ, Foo DY, Cerutti PA, Fusenig NE. 1990. c-Ha-ras oncogene expression in immortalized human keratinocytes(HaCaT) alters growth potential in vivo but lacks correlation with malignancy. Cancer Res 50:2840–2847.

Boukamp P, Popp S, Altmeyer S, Hülsen A, Fasching C, Cremer T, Fusenig NE. 1997. Sustained nontumorigenic phenotype correlates with a largely stable chromosome content during long-term culture of the human keratinocyte line HaCaT. Genes Chromosomes Cancer 19:201–214.

Breitkreutz D, Boukamp P, Ryle CM, Stark HJ, Roop DR, Fusenig NE. 1991. Epidermal morphogenesis and keratin expression in c-Ha-ras-transfected tumorigenic clones of the human HaCaT cell line. Cancer Res 51:4402–4409.

Breitkreutz D, Stark HJ, Mirancea N, Tomakidi P, Steinbauer H, Fusenig NE. 1997. Integrin and basement membrane normalization in mouse grafts of human keratinocytes-implications for epidermal homeostasis. Differentiation 61:195–209.

Brock HW, van Lohuizen M. 2001. The Polycomb group-no longer an exclusive club? Curr Opin Genet Dev 11:175–181.

Chiba T, Zheng YW, Kita K, Yokosuka O, Saisho H, Onodera M, Miyoshi H, Nakano M, Zen Y, Nakanuma Y, Nakauchi H, Iwama A, Taniguchi H. 2007. Enhanced self-renewal capability in hepatic stem/progenitor cells drives cancer initiation. Gastroenterology 133:937–950.

Dimri GP, Martinez JL, Jacobs JJ, Keblusek P, Itahana K, Van Lohuizen M, Campisi J, Wazer DE, Band V. 2002. The Bmi-1 oncogene induces telomerase activity and immortalizes human mammary epithelial cells. Cancer Res 62:4736–4745.

Ehrhart JC, Gosselet FP, Culerrier RM, Sarasin A. 2003. UVB-induced mutations in human key gatekeeper genes governing signalling pathways and consequences for skin tumourigenesis. Photochem Photobiol Sci 2:825–834.

Francis NJ, Kingston RE. 2001. Mechanisms of transcriptional memory. Nat Rev Mol Cell Biol 2:409–421.

Fusenig NE. 1994. Epithelial-mesenchymal interactions regulate keratinocyte growth and differentiation in vitro. In: Leigh I, Lane B, Watt F, editors. The keratinocyte handbook. New York: Cambridge University Press. pp 71–94.

Fusenig NE, Boukamp P. 1998. Multiple stages and genetic alterations in immortalization, malignant transformation, and tumor progression of human skin keratinocytes. Mol Carcinog 23:144–158.

Fusenig NE, Breitkreutz D, Dzarlieva RT, Boukamp P, Bohnert A, Tilgen W. 1983. Growth and differentiation characteristics of transformed keratinocytes from mouse and human skin in vitro and in vivo. J Invest Dermatol 81:168s–175s.

Fusenig NE, Dzarlieva-Petrusevska RT, Breitkreutz D. 1985. Phenotypic and cytogenetic characteristics of different stages during spontaneous transformation of mouse keratinocytes in vitro. Carcinog Compr Surv 9:293–326.

Haupt Y, Alexander WS, Barri G, Klinken SP, Adams JM. 1991. Novel zinc finger gene implicated as myc collaborator by retrovirally accelerated lymphomagenesis in E mu-myc transgenic mice. Cell 65:753–763.

Jamieson CH, Ailles LE, Dylla SJ, Muijtjens M, Jones C, Zehnder JL, Gotlib J, Li K, Manz MG, Keating A, Sawyers CL, Weissman IL. 2004. Granulocyte-macrophage progenitors as candidate leukemic stem cells in blast-crisis CML. N Engl J Med 351:657–667.

Kim JH, Yoon SY, Kim CN, Joo JH, Moon SK, Choe IS, Choe YK, Kim JW. 2004. The Bmi-1 oncoprotein is overexpressed in human colorectal cancer and correlates with the reduced p16INK4a/p14ARF proteins. Cancer Lett 203:217–224.

Lacour JP. 2002. Carcinogenesis of basal cell carcinomas:genetics and molecular mechanisms. Br J Dermatol 61:17–19.

Lapidot T, Sirard C, Vormoor J, Murdoch B, Hoang T, Caceres-Cortes J, Minden M, Paterson B, Caligiuri MA, Dick JE. 1994. A cell initiating human acute myeloid leukaemia after transplantation into SCID mice. Nature 367:645–648.

Lessard J, Sauvageau G. 2003. Bmi-1 determines the proliferative capacity of normal and leukaemic stem cells. Nautre 423:255–260.

Leung C, Lingbeek M, Shakhova O, Liu J, Tanger E, Saremaslani P, Van Lohuizen M, Marino S. 2004. Bmi1 is essential for cerebellar development and is overexpressed in human medulloblastomas. Nature 428:337–341.

Lindström MS, Klangby U, Wiman KG. 2001. p14ARF homozygous deletion or MDM2 overexpression in Burkitt lymphoma lines carrying wild type p53. Oncogene 20:2171–2177.

Lipinski MM, Jacks T. 1999. The retinoblastoma gene family in differentiation and development. Oncogene 18:7873–7882.

Lowe SW, Sherr CJ. 2003. Tumor suppression by Ink4a-Arf: Progress and puzzles. Curr Opin Genet Dev 13:77–83.

Lukas J, Parry D, Aagaard L, Mann DJ, Bartkova J, Strauss M, Peters G, Bartek J. 1995. Retinoblastoma-protein-dependent cell-cycle inhibition by the tumour suppressor p16. Nature 375:503–506.

Molofsky AV, Pardal R, Iwashita T, Park IK, Clarke MF, Morrison SJ. 2003. Bmi-1 dependence distinguishes neural stem cell self-renewal from progenitor proliferation. Nature 425:962–967.

Park IK, Qian D, Kiel M, Becker MW, Pihalja M, Weissman IL, Morrison SJ, Clarke MF. 2003. Bmi-1 is required for maintenance of adult self-renewing haematopoietic stem cells. Nature 423:302–305.

Park IK, Morrison SJ, Clarke MF. 2004. Bmi1, stem cells, and senescence regulation. J Clin Invest 113:175–179.

Pomerantz J, Schreiber-Agus N, Liégeois NJ, Silverman A, Alland L, Chin L, Potes J, Chen K, Orlow I, Lee HW, Cordon-Cardo C, DePinho RA. 1998. The Ink4a tumor suppressor gene product, p19Arf, interacts with MDM2 and neutralizes MDM2's inhibition of p53. Cell 92:713–723.

Raaphorst FM, van Kemenade FJ, Blokzijl T, Fieret E, Hamer KM, Satijn DP, Otte AP, Meijer CJ. 2000. Coexpression of BMI-1 and EZH2 polycomb group genes in Reed-Sternberg cells of Hodgkin's disease. Am J Pathol 157:709–715.

Reinisch CM, Uthman A, Erovic BM, Pammer J. 2007. Expression of BMI-1 in normal skin and inflammatory and neoplastic skin lesions. J Cutan Pathol 34:174–180.

Ringrose L, Paro R. 2001. Remembering silence. BioEssays 23:566–570.

Saxon PJ, Srivatsan ES, Leipzig GV, Sameshima JH, Stanbridge EJ. 1985. Selective transfer of individual human chromosomes to recipient cells. Mol Cell Biol 5:140–146.

Sharpless NE, DePinho RA. 1999. The INK4A/ARF locus and its two gene products. Curr Opin Genet Dev 9:22–30.

Singh SK, Clarke ID, Terasaki M, Bonn VE, Hawkins C, Squire J, Dirks PB. 2003. Identification of a cancer stem cell in human brain tumor. Cancer Res 63:5821–5828.

van der Lugt NM, Domen J, Linders K, van Roon M, Robanus-Maandag E, te Riele H, van der Valk M, Deschamps J, Sofroniew M, van Lohuizen M. 1994. Posterior transformation, neurological abnormalities, and severe hematopoietic defects in mice with a targeted deletion of the bmi-1 proto-oncogene. Genes Dev 8:757–769.

van Kemenade FJ, Raaphorst FM, Blokzijl T, Fieret E, Hamer KM, Satijn DP, Otte AP, Meijer CJ. 2001. Coexpression of BMI-1 and EZH2 polycomb-group proteins is associated with cycling cells and degree of malignancy in B-cell non-Hodgkin lymphoma. Blood 97:3896–3901.

van Lohuizen M, Frasch M, Wientjens E, Berns A. 1991. Sequence similarity between the mammalian bmi-1 proto-oncogene and the Drosophila regulatory genes Psc and Su(z)2. Nautre 353:353–355.

Varambally S, Dhanasekaran SM, Zhou M, Barrette TR, Kumar-Sinha C, Sanda MG, Ghosh D, Pienta KJ, Sewalt RG, Otte AP, Rubin MA, Chinnaiyan AM. 2002. The polycomb group protein EZH2 is involved in progression of prostate cancer. Nature 419:624–629.

Visser HP, Gunster MJ, Kluin-Nelemans HC, Manders EM, Raaphorst FM, Meijer CJ, Willemze R, Otte AP. 2001. The polycomb group protein EZH2 is upregulated in proliferating, cultured human mantle cell lymphoma. Br J Haematol 112:950–958.

Vonlanthen S, Heighway J, Altermatt HJ, Gugger M, Kappeler A, Borner MM, van Lohuizen M, Betticher DC. 2001. The bmi-1 oncoprotein is differentially expressed in non-small cell lung cancer and correlates with INK4A-ARF locus expression. Br J Cancer 84:1372–1376.

Wang H, Pan K, Zhang HK, Weng DS, Zhou J, Li JJ, Huang W, Song HF, Chen MS, Xia JC. 2008. Increased polycomb-group oncogene Bmi-1 expression correlates with poor prognosis in hepatocellular carcinoma. J Cancer Res Clin Oncol 134:535–541.

Weber JD, Taylor LJ, Roussel MF, Sherr CJ, Bar-Sagi D. 1999. Nucleolar Arf sequesters Mdm2 and activates p53. Nat Cell Biol 1:20–26.

Wicha MS, Liu S, Dontu G. 2006. Cancer stem cells: An old idea—a paradigm shift. Cancer Res 66:1883–1890.

Zhang Y, Xiong Y, Yarbrough WG. 1998. ARF promotes MDM2 degradation and stabilizes p53: ARF-INK4a locus deletion impairs both the Rb and p53 tumour suppression pathways. Cell 92:725–734.